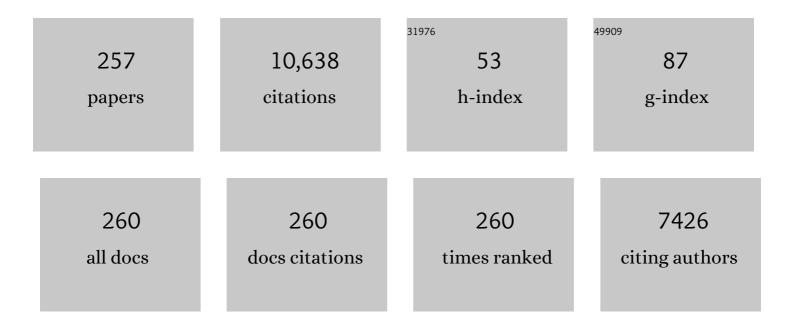
List of Publications by Year in descending order

Source: https://exaly.com/author-pdf/8231314/publications.pdf Version: 2024-02-01



#	Article	IF	CITATIONS
1	Efficient synthesis of bioetheric fuel additive by combining the reductive and direct etherification of furfural in one-pot over Pd nanoparticles deposited on zeolites. Green Energy and Environment, 2023, 8, 519-529.	8.7	4
2	Intra-crystalline mesoporous zeolite encapsulation-derived thermally robust metal nanocatalyst in deep oxidation of light alkanes. Nature Communications, 2022, 13, 295.	12.8	54
3	Hydrated Hydroxide Complex Dominates the AIE Properties of Nonconjugated Polymeric Luminophores. Macromolecular Rapid Communications, 2022, 43, e2100720.	3.9	11
4	One-pot conversion of dimethyl terephthalate to 1,4-cyclohexanedimethanol. Applied Catalysis A: General, 2022, 632, 118510.	4.3	7
5	DNAâ€Assisted Creation of a Library of Ultrasmall Multimetal/Metal Oxide Nanoparticles Confined in Silica. Small, 2022, 18, e2107123.	10.0	3
6	New progress in zeolite synthesis and catalysis. National Science Review, 2022, 9, .	9.5	43
7	"Burr Puzzle―Like Hierarchical Beta zeolite composed of crisscrossed nanorods. Microporous and Mesoporous Materials, 2022, 335, 111843.	4.4	6
8	Synthesis of Micro-Mesoporous Ti-MOR/Silica Composite Spheres in Oil-in-water Microemulsion System. Chemical Research in Chinese Universities, 2022, 38, 192-199.	2.6	5
9	Stacking-faulted CDO zeolite nanosheets efficient for bulky molecular reactions. Chemical Communications, 2022, 58, 6008-6011.	4.1	1
10	Highly Hydrophilic Tiâ^'Beta Zeolite with Tiâ^'Rich Exterior as Efficient Catalyst for Cyclohexene Epoxidation. Catalysts, 2022, 12, 434.	3.5	3
11	Structural Transformation-Involved Synthesis of Nanosized ERI-Type Zeolite and Its Catalytic Property in the MTO Reaction. Inorganic Chemistry, 2022, 61, 8066-8075.	4.0	4
12	New CHA-Type aluminoborosilicates as efficient catalysts for MTO and NH3-SCR of NOx reactions. Chemical Engineering Journal, 2022, 444, 136657.	12.7	4
13	Aluminum sulphate-assisted stepwise dealumination of OSDA-free low-silica chabazite for methanol-to-olefin reaction. Microporous and Mesoporous Materials, 2022, 338, 111972.	4.4	2
14	Preparation of a cost-effective Ni–Ag bimetallic catalyst for hydrodehalogenation of aryl halides under mild conditions. New Journal of Chemistry, 2022, 46, 12169-12176.	2.8	1
15	Direct Synthesis and Delamination of Swollen Layered Ferrierite for the Reductive Etherification of Furfural. ChemCatChem, 2022, 14, .	3.7	3
16	Investigation of the active centers and structural modifications for TS-1 in catalyzing the Beckmann rearrangement. Catalysis Today, 2022, 405-406, 193-202.	4.4	6
17	Preparation of trimetallic electrocatalysts by one-step co-electrodeposition and efficient CO <sub>2</sub> reduction to ethylene. Chemical Science, 2022, 13, 7509-7515.	7.4	5
18	Topotactic conversion of Ge-rich IWW zeolite into IPC-18 under mild condition. Microporous and Mesoporous Materials, 2021, 310, 110617.	4.4	13

#	Article	IF	CITATIONS
19	Hierarchical Ti-Beta zeolites with uniform intracrystalline mesopores hydrothermally synthesized via interzeolite transformation for oxidative desulfurization. Microporous and Mesoporous Materials, 2021, 311, 110702.	4.4	19
20	Selective synthesis of epichlorohydrin <i>via</i> liquid-phase allyl chloride epoxidation over a modified Ti-MWW zeolite in a continuous slurry bed reactor. New Journal of Chemistry, 2021, 45, 331-342.	2.8	9
21	Selective hydrogenation of cinnamaldehyde with Ni Fe1-Al2O4+ composite oxides supported Pt catalysts: C O versus C C selectivity switch by varying the Ni/Fe molar ratios. Journal of Catalysis, 2021, 393, 126-139.	6.2	35
22	Postsynthesis of high silica beta by cannibalistic dealumination of OSDA-free beta and its catalytic applications. Inorganic Chemistry Frontiers, 2021, 8, 1574-1587.	6.0	7
23	Al-Modified Ti-MOR as a robust catalyst for cyclohexanone ammoximation with enhanced anti-corrosion performance. Catalysis Science and Technology, 2021, 11, 7287-7299.	4.1	8
24	K <sup>+</sup> located in 6-membered rings of low-silica CHA enhancing the lifetime and propene selectivity in MTO. Catalysis Science and Technology, 2021, 11, 6234-6247.	4.1	4
25	Designing SAPO-18 with energetically favorable tetrahedral Si ions for an MTO reaction. Chemical Communications, 2021, 57, 5682-5685.	4.1	6
26	Synthesis of cyclohexanol and ethanol <i>via</i> the hydrogenation of cyclohexyl acetate with Cu <sub>2</sub> Zn <sub><i>x</i></sub> /Al <sub>2</sub> O <sub>3</sub> catalysts. Catalysis Science and Technology, 2021, 11, 7035-7046.	4.1	8
27	Extra-Large Pore Titanosilicate Synthesized via Reversible 3D–2D–3D Structural Transformation as Highly Active Catalyst for Cycloalkene Epoxidation. ACS Catalysis, 2021, 11, 2650-2662.	11.2	17
28	Ultrafast synthesis of high-silica Beta zeolite from dealuminated MOR by interzeolite transformation for methanol to propylene reactions. Microporous and Mesoporous Materials, 2021, 314, 110894.	4.4	6
29	Bimetallic Pt-Fe catalysts supported on mesoporous TS-1 microspheres for the liquid-phase selective hydrogenation of cinnamaldehyde. Journal of Catalysis, 2021, 395, 375-386.	6.2	25
30	Two-dimensional zeolites in catalysis: current state-of-the-art and perspectives. Catalysis Reviews - Science and Engineering, 2021, 63, 234-301.	12.9	11
31	Library Creation of Ultrasmall Multiâ€metallic Nanoparticles Confined in Mesoporous MFI Zeolites. Angewandte Chemie, 2021, 133, 14692-14698.	2.0	4
32	Library Creation of Ultrasmall Multiâ€netallic Nanoparticles Confined in Mesoporous MFI Zeolites. Angewandte Chemie - International Edition, 2021, 60, 14571-14577.	13.8	11
33	Efficient Synthesis of Cyclohexanol and Ethanol via the Hydrogenation of Acetic Acidâ€Derived Cyclohexyl Acetate with the Cu <sub>x</sub> Al <sub>1</sub> Mn <sub>2â^'x</sub> Catalysts. ChemCatChem, 2021, 13, 3099-3111.	3.7	5
34	Skeleton-Sn anchoring isolated Pt site to confine subnanometric clusters within *BEA topology. Journal of Catalysis, 2021, 397, 44-57.	6.2	36
35	Surface Molecule Manipulated Pt/TiO <sub>2</sub> Catalysts for Selective Hydrogenation of Cinnamaldehyde. Journal of Physical Chemistry C, 2021, 125, 13304-13312.	3.1	21
36	Selective conversion of methanol to propylene over highly dealuminated mordenite: Al location and crystal morphology effects. Chinese Journal of Catalysis, 2021, 42, 1147-1159.	14.0	16

#	Article	IF	CITATIONS
37	Continuous hydrogenation of CO2-derived ethylene carbonate to methanol and ethylene glycol at Cu-MoOx interface with a low H2/ester ratio. Journal of Catalysis, 2021, 399, 98-110.	6.2	22
38	Two Coexisting Forms of Simple Molecules for Directing Sesqui-Unit-Cell Zeolite Nanosheets. Chemistry of Materials, 2021, 33, 6934-6941.	6.7	11
39	Structured binder-free MWW-type titanosilicate with Si-rich shell for selective and durable propylene epoxidation. Chinese Journal of Catalysis, 2021, 42, 1561-1575.	14.0	12
40	Cost-effective fast-synthesis of chabazite zeolites for the reduction of NOx. Applied Catalysis B: Environmental, 2021, 292, 120163.	20.2	37
41	Expanded titanosilicate MWW-related materials synthesized from a boron-containing precursor as an efficient catalyst for cyclohexene oxidation. Microporous and Mesoporous Materials, 2021, 327, 111437.	4.4	3
42	Zeolites featuring 14 × 12-ring channels with unique adsorption properties. Inorganic Chemistry Frontiers, 2021, 8, 5277-5285.	6.0	5
43	"Open―Nonporous Nonasil Zeolite Structure for Selective Catalysis. Journal of the American Chemical Society, 2021, 143, 20569-20573.	13.7	14
44	Comparison of titanosilicates with different topologies as liquid-phase oxidation catalysts. Catalysis Today, 2020, 347, 48-55.	4.4	9
45	One-pot synthesis of layered mesoporous ZSM-5 plus Cu ion-exchange: Enhanced NH3-SCR performance on Cu-ZSM-5 with hierarchical pore structures. Journal of Hazardous Materials, 2020, 385, 121593.	12.4	87
46	3D Electron Diffraction Unravels the New Zeolite ECNUâ€23 from the "Pure―Powder Sample of ECNUâ€21. Angewandte Chemie, 2020, 132, 1182-1186.	2.0	8
47	3D Electron Diffraction Unravels the New Zeolite ECNUâ€23 from the "Pure―Powder Sample of ECNUâ€21. Angewandte Chemie - International Edition, 2020, 59, 1166-1170.	13.8	27
48	Efficient liquid-phase hydrogenation of cinnamaldehyde to cinnamyl alcohol with a robust PtFe/HPZSM-5 catalyst. Journal of Catalysis, 2020, 382, 1-12.	6.2	46
49	Host-guest chemistry immobilized nickel nanoparticles on zeolites as efficient catalysts for amination of 1-octanol. Journal of Catalysis, 2020, 381, 443-453.	6.2	19
50	Hierarchical three-dimensionally ordered macroporous Fe-V binary metal oxide catalyst for low temperature selective catalytic reduction of NOx from marine diesel engine exhaust. Applied Catalysis B: Environmental, 2020, 268, 118455.	20.2	44
51	Modified Ti-MWW Zeolite as a Highly Efficient Catalyst for the Cyclopentene Epoxidation Reaction. Frontiers in Chemistry, 2020, 8, 585347.	3.6	6
52	Electrodeposited Cu–Pd bimetallic catalysts for the selective electroreduction of CO <sub>2</sub> to ethylene. Green Chemistry, 2020, 22, 7560-7565.	9.0	30
53	Highly selective 1-pentene epoxidation over Ti-MWW with modified microenvironment of Ti active sites. Catalysis Science and Technology, 2020, 10, 6050-6064.	4.1	22

#	Article	lF	CITATIONS
55	Environmental benign synthesis of Nano-SSZ-13 via FAU trans-crystallization: Enhanced NH3-SCR performance on Cu-SSZ-13 with nano-size effect. Journal of Hazardous Materials, 2020, 398, 122986.	12.4	58
56	Efficient synthesis of methanol and ethylene glycol <i>via</i> the hydrogenation of CO <sub>2</sub> -derived ethylene carbonate on Cu/SiO <sub>2</sub> catalysts with balanced Cu <sup>+</sup> –Cu <sup>0</sup> sites. Catalysis Science and Technology, 2020, 10, 5149-5162.	4.1	33
57	ECNUâ€36: A Quasiâ€Pure Polymorph C H Beta Silicate Composed of Hierarchical Nanosheet Crystals for Effective VOCs Adsorption. Angewandte Chemie, 2020, 132, 17444-17449.	2.0	1
58	ECNUâ€36: A Quasiâ€Pure Polymorph C <sub>H</sub> Beta Silicate Composed of Hierarchical Nanosheet Crystals for Effective VOCs Adsorption. Angewandte Chemie - International Edition, 2020, 59, 17291-17296.	13.8	17
59	Postsynthesis of Ti-UZM-35 titanosilicate as efficient catalyst for phenol hydroxylation reaction. Microporous and Mesoporous Materials, 2020, 305, 110321.	4.4	8
60	Oxidative desulfurization of model oil over Ta-Beta zeolite synthesized via structural reconstruction. Journal of Hazardous Materials, 2020, 393, 122458.	12.4	20
61	Deboronation-assisted construction of defective Ti(OSi) <sub>3</sub> OH species in MWW-type titanosilicate and their enhanced catalytic performance. Catalysis Science and Technology, 2020, 10, 2905-2915.	4.1	25
62	Hydrothermal synthesis of boron-free Zr-MWW and Sn-MWW zeolites as robust Lewis acid catalysts. Chemical Communications, 2020, 56, 4696-4699.	4.1	10
63	Origin of the Photoluminescence of Metal Nanoclusters: From Metal-Centered Emission to Ligand-Centered Emission. Nanomaterials, 2020, 10, 261.	4.1	137
64	High Ethylene Selectivity in Methanolâ€ŧoâ€Olefin (MTO) Reaction over MORâ€Zeolite Nanosheets. Angewandte Chemie - International Edition, 2020, 59, 6258-6262.	13.8	46
65	High Ethylene Selectivity in Methanolâ€toâ€Olefin (MTO) Reaction over MORâ€Zeolite Nanosheets. Angewandte Chemie, 2020, 132, 6317-6321.	2.0	33
66	Postsynthesis of hierarchical core/shell ZSM-5 as an efficient catalyst in ketalation and acetalization reactions. Frontiers of Chemical Science and Engineering, 2020, 14, 258-266.	4.4	6
67	Novel shielding and synergy effects of Mn-Ce oxides confined in mesoporous zeolite for low temperature selective catalytic reduction of NOx with enhanced SO2/H2O tolerance. Journal of Hazardous Materials, 2020, 396, 122592.	12.4	79
68	Hierarchical zeolite enveloping Pd-CeO2 nanowires: An efficient adsorption/catalysis bifunctional catalyst for low temperature propane total degradation. Chemical Engineering Journal, 2020, 393, 124717.	12.7	62
69	Spatial and chemical confined ultra-small CsPbBr3 perovskites in dendritic mesoporous silica nanospheres with enhanced stability. Microporous and Mesoporous Materials, 2020, 302, 110229.	4.4	19
70	Efficient electrocatalytic reduction of carbon dioxide to ethylene on copper–antimony bimetallic alloy catalyst. Chinese Journal of Catalysis, 2020, 41, 1091-1098.	14.0	39
71	Relation of Selective Oxidation Catalytic Performance to Microenvironment of Ti <sup>IV</sup> Active Site Based on Isotopic Labeling. ACS Catalysis, 2020, 10, 4813-4819.	11.2	34
72	SBAâ€15 Supported Chiral Phosphineâ€Gold(I) Complex: Highly Efficient and Recyclable Catalyst for Asymmetric Cycloaddition Reactions. ChemCatChem, 2020, 12, 4067-4072.	3.7	7

#	Article	IF	CITATIONS
73	Total Hydrogenation of Furfural under Mild Conditions over a Durable Ni/TiO-SiO Catalyst with Amorphous TiO Species. ACS Omega, 2020, 5, 30257-30266.	3.5	0
74	Total Hydrogenation of Furfural under Mild Conditions over a Durable Ni/TiO <sub>2</sub> –SiO <sub>2</sub> Catalyst with Amorphous TiO <sub>2</sub> Species. ACS Omega, 2020, 5, 30257-30266.	3.5	12
75	One-pot co-condensation strategy for dendritic mesoporous organosilica nanospheres with fine size and morphology control. CrystEngComm, 2019, 21, 4030-4035.	2.6	27
76	Mechanism of Photoluminescence in Ag Nanoclusters: Metal-Centered Emission versus Synergistic Effect in Ligand-Centered Emission. Journal of Physical Chemistry C, 2019, 123, 18638-18645.	3.1	33
77	Size-Controlled Growth of Silver Nanoparticles onto Functionalized Ordered Mesoporous Polymers for Efficient CO <sub>2</sub> Upgrading. ACS Applied Materials & Interfaces, 2019, 11, 44241-44248.	8.0	19
78	Co Fe1-Al2O4+ composite oxides supported Pt nanoparticles as efficient and recyclable catalysts for the liquid-phase selective hydrogenation of cinnamaldehyde. Journal of Catalysis, 2019, 380, 254-266.	6.2	32
79	One-pot synthesized core/shell structured zeolite@copper catalysts for selective hydrogenation of ethylene carbonate to methanol and ethylene glycol. Green Chemistry, 2019, 21, 5414-5426.	9.0	31
80	Doping Pd/SiO <sub>2</sub> with Na <sup>+</sup> : changing the reductive etherification of Cî€O to furan ring hydrogenation of furfural in ethanol. RSC Advances, 2019, 9, 25345-25350.	3.6	10
81	Highly tunable periodic imidazole-based mesoporous polymers as cooperative catalysts for efficient carbon dioxide fixation. Catalysis Science and Technology, 2019, 9, 1030-1038.	4.1	23
82	Topotactic Conversion of Alkaliâ€Treated Intergrown Germanosilicate CITâ€13 into Singleâ€Crystalline ECNUâ€21 Zeolite as Shapeâ€Selective Catalyst for Ethylene Oxide Hydration. Chemistry - A European Journal, 2019, 25, 4520-4529.	3.3	51
83	Structural reconstruction of germanosilicate frameworks by controlled hydrogen reduction. Chemical Communications, 2019, 55, 1883-1886.	4.1	10
84	Catalysts in Coronas: A Surface Spatial Confinement Strategy for High-Performance Catalysts in Methane Dry Reforming. ACS Catalysis, 2019, 9, 9072-9080.	11.2	121
85	Active and stable Pt-Ceria nanowires@silica shell catalyst: Design, formation mechanism and total oxidation of CO and toluene. Applied Catalysis B: Environmental, 2019, 256, 117807.	20.2	57
86	Sn-doped Pt catalyst supported on hierarchical porous ZSM-5 for the liquid-phase hydrogenation of cinnamaldehyde. Catalysis Science and Technology, 2019, 9, 3226-3237.	4.1	36
87	Exploring the Nanosize Effect of Mordenite Zeolites on Their Performance in the Removal of NO <sub><i>x</i></sub> . Industrial & Engineering Chemistry Research, 2019, 58, 8625-8635.	3.7	18
88	Ultrafast synthesis of nanosized Ti-Beta as an efficient oxidation catalyst <i>via</i> a structural reconstruction method. Catalysis Science and Technology, 2019, 9, 1857-1866.	4.1	27
89	Pt nanoparticles supported on YCo <sub>x</sub> Fe <sub>1â^'x</sub> O <sub>3</sub> perovskite oxides: highly efficient catalysts for liquid-phase hydrogenation of cinnamaldehyde. Chemical Communications, 2019, 55, 3363-3366.	4.1	33
90	P band intermediate state (PBIS) tailors photoluminescence emission at confined nanoscale interface. Communications Chemistry, 2019, 2, .	4.5	27

#	Article	IF	CITATIONS
91	Intensified interzeolite transformation: ultrafast synthesis of active and stable Ti-Beta zeolites without solvents. Chemical Communications, 2019, 55, 14279-14282.	4.1	33
92	An efficient Cu-based catalyst for the hydrogenation of ethylene carbonate to ethylene glycol and methanol. Catalysis Science and Technology, 2019, 9, 6749-6759.	4.1	21
93	Controllably Confined ZnO on USY Zeolites (USY@ZnO/Al <sub>2</sub> O <sub>3</sub> ) as Efficient Lewis Acid Catalysts for Baeyer–Villiger Oxidation. Chemistry - an Asian Journal, 2018, 13, 1213-1222.	3.3	2
94	Understanding the oxidative dehydrogenation of ethyl lactate to ethyl pyruvate over vanadia/titania. Catalysis Science and Technology, 2018, 8, 3737-3747.	4.1	31
95	In Situ Embedded Pseudo Pd–Sn Solid Solution in Micropores Silica with Remarkable Catalytic Performance for CO and Propane Oxidation. ACS Applied Materials & Interfaces, 2018, 10, 9220-9224.	8.0	42
96	Sn-Beta zeolite derived from a precursor synthesized via an organotemplate-free route as efficient Lewis acid catalyst. Applied Catalysis A: General, 2018, 556, 52-63.	4.3	15
97	Bolaform Molecules Directing Intergrown Zeolites. Journal of Physical Chemistry C, 2018, 122, 9117-9126.	3.1	10
98	Total Hydrogenation of Furfural over Pd/Al <sub>2</sub> O <sub>3</sub> and Ru/ZrO <sub>2</sub> Mixture under Mild Conditions: Essential Role of Tetrahydrofurfural as an Intermediate and Support Effect. ACS Sustainable Chemistry and Engineering, 2018, 6, 6957-6964.	6.7	63
99	Cu–Mg–Zr/SiO <sub>2</sub> catalyst for the selective hydrogenation of ethylene carbonate to methanol and ethylene glycol. Catalysis Science and Technology, 2018, 8, 2624-2635.	4.1	29
100	Mesoporous MFI Zeolite with a 2D Square Structure Directed by Surfactants with an Azobenzene Tail Group. Chemistry - A European Journal, 2018, 24, 8615-8623.	3.3	18
101	Hierarchical ZSM-5 nanocrystal aggregates: seed-induced green synthesis and its application in alkylation of phenol with <i>tert</i> -butanol. RSC Advances, 2018, 8, 2751-2758.	3.6	28
102	One-pot synthesis of ethylene glycol by oxidative hydration of ethylene with hydrogen peroxide over titanosilicate catalysts. Journal of Catalysis, 2018, 358, 89-99.	6.2	55
103	Highly efficient mesoporous polymer supported phosphine-gold( <scp>i</scp> ) complex catalysts for amination of allylic alcohols and intramolecular cyclization reactions. RSC Advances, 2018, 8, 1737-1743.	3.6	10
104	Synthesis of Largeâ€Pore ECNUâ€19 Material (12 × 8â€R) <i>via</i> Interlayerâ€Expansion of HUSâ€2 Lamellar Silicate. Chinese Journal of Chemistry, 2018, 36, 227-232.	4.9	8
105	Highly Selective Oxidation of Ethyl Lactate to Ethyl Pyruvate Catalyzed by Mesoporous Vanadia–Titania. ACS Catalysis, 2018, 8, 2365-2374.	11.2	38
106	Synthesis of ultra-small mordenite zeolite nanoparticles. Science China Materials, 2018, 61, 1185-1190.	6.3	10
107	Facile synthesis of furfuryl ethyl ether in high yield <i>via</i> the reductive etherification of furfural in ethanol over Pd/C under mild conditions. Green Chemistry, 2018, 20, 2110-2117.	9.0	47
108	Pore size-tunable titanosilicates post-synthesized from germanosilicate by structural reorganization and H2TiF6-assisted isomorphous substitution. Applied Catalysis A: General, 2018, 550, 11-19.	4.3	32

#	Article	IF	CITATIONS
109	A Hierarchical MFI Zeolite with a Twoâ€Dimensional Square Mesostructure. Angewandte Chemie - International Edition, 2018, 57, 724-728.	13.8	67
110	Dendritic and Core–Shell–Corona Mesoporous Sister Nanospheres from Polymer–Surfactant–Silica Selfâ€Entanglement. Chemistry - A European Journal, 2018, 24, 478-486.	3.3	19
111	At room temperature in water: efficient hydrogenation of furfural to furfuryl alcohol with a Pt/SiC–C catalyst. RSC Advances, 2018, 8, 37243-37253.	3.6	21
112	Size-Dependent Catalytic Activity of Oxo-Hydroxo Titanium Sub-Nanoislets Grafted on Organically Modified Mesoporous Silica. Langmuir, 2018, 34, 12713-12722.	3.5	5
113	Hierarchical MFI Zeolites with a Singleâ€Crystalline Spongeâ€Like Mesostructure. Chemistry - A European Journal, 2018, 24, 19300-19308.	3.3	6
114	Design and Synthesis of Cu/ZSM-5 Catalyst via a Facile One-Pot Dual-Template Strategy with Controllable Cu Content for Removal of NO <sub><i>x</i></sub> . Industrial & Engineering Chemistry Research, 2018, 57, 14967-14976.	3.7	35
115	Synthesis of Ethylâ€4â€ethoxy Pentanoate by Reductive Etherification of Ethyl Levulinate in Ethanol on Pd/SiO <sub>2</sub> â€C Catalysts. ChemSusChem, 2018, 11, 3796-3802.	6.8	5
116	Crystallization of a Novel Germanosilicate ECNUâ€16 Provides Insights into the Spaceâ€Filling Effect on Zeolite Crystal Symmetry. Chemistry - A European Journal, 2018, 24, 9247-9253.	3.3	11
117	Freestanding Cobaltâ€Aluminum Oxides on USY Zeolite as an Efficient Catalyst for Selective Catalytic Reduction of NO <sub><i>x</i></sub> . ChemCatChem, 2018, 10, 4074-4083.	3.7	11
118	Design of Stable Ultrasmall Ptâ^'Ni(O) Nanoparticles with Enhanced Catalytic Performance: Insights into the Effects of Ptâ^'Niâ^'NiO Dual Interfaces. ChemCatChem, 2018, 10, 4134-4142.	3.7	12
119	Hydrothermal synthesis of Sn-Beta zeolites in F <sup>â^'</sup> -free medium. Inorganic Chemistry Frontiers, 2018, 5, 2763-2771.	6.0	20
120	Highly Efficient Electroreduction of CO <sub>2</sub> to Methanol on Palladium–Copper Bimetallic Aerogels. Angewandte Chemie - International Edition, 2018, 57, 14149-14153.	13.8	222
121	Synthesis of Extraâ€Largeâ€Pore Zeolite ECNUâ€9 with Intersecting 14*12â€Ring Channels. Angewandte Chemie International Edition, 2018, 57, 9515-9519.	13.8	29
122	Breaking Structural Energy Constraints: Hydrothermal Crystallization of Highâ€Silica Germanosilicates by a Buildingâ€Unit Selfâ€Growth Approach. Chemistry - A European Journal, 2018, 24, 13297-13305.	3.3	12
123	Synthesis of Extraâ€Largeâ€Pore Zeolite ECNUâ€9 with Intersecting 14*12â€Ring Channels. Angewandte Chemie 2018, 130, 9659-9663.	<sup>2</sup> , 2.0	7
124	An amphiphilic composite material of titanosilicate@mesosilica/carbon as a Pickering catalyst. Chemical Communications, 2018, 54, 7932-7935.	4.1	22
125	Controllable hydrothermal synthesis of Ni/H-BEA with a hierarchical core–shell structure and highly enhanced biomass hydrodeoxygenation performance. Nanoscale, 2017, 9, 5986-5995.	5.6	32
126	Facile Synthesis of Ethyl-4-ethoxy Pentanoate as a Novel Biofuel Additive Derived from γ-Valerolactone. ACS Sustainable Chemistry and Engineering, 2017, 5, 6645-6653.	6.7	9

#	Article	IF	CITATIONS
127	Sn-Beta zeolite hydrothermally synthesized via interzeolite transformation as efficient Lewis acid catalyst. Journal of Catalysis, 2017, 352, 1-12.	6.2	88
128	Enhancing ethylene epoxidation of a MWW-type titanosilicate/H2O2 catalytic system by fluorine implanting. Catalysis Science and Technology, 2017, 7, 2624-2631.	4.1	28
129	Simple CTAB surfactant-assisted hierarchical lamellar MWW titanosilicate: a high-performance catalyst for selective oxidations involving bulky substrates. Catalysis Science and Technology, 2017, 7, 2874-2885.	4.1	28
130	Fast synthesis of hierarchical Beta zeolites with uniform nanocrystals from layered silicate precursor. Microporous and Mesoporous Materials, 2017, 248, 30-39.	4.4	46
131	Recent Progresses in Titanosilicates. Chinese Journal of Chemistry, 2017, 35, 836-844.	4.9	26
132	Synthesis of two titanosilicates with distinct interlayer connections from similar gels. Dalton Transactions, 2017, 46, 5776-5780.	3.3	4
133	A dual-templating strategy for the scale-up synthesis of dendritic mesoporous silica nanospheres. Green Chemistry, 2017, 19, 5575-5581.	9.0	58
134	Structural reconstruction: a milestone in the hydrothermal synthesis of highly active Sn-Beta zeolites. Chemical Communications, 2017, 53, 12516-12519.	4.1	34
135	Facile synthesis of ECNU-20 (IWR) hollow sphere zeolite composed of aggregated nanosheets. Dalton Transactions, 2017, 46, 15641-15645.	3.3	12
136	Robust synthesis of green fuels from biomass-derived ethyl esters over a hierarchically core/shell-structured ZSM-5@(Co/SiO <sub>2</sub> ) catalyst. Chemical Communications, 2017, 53, 10172-10175.	4.1	15
137	Clean synthesis of furfural oxime through liquid-phase ammoximation of furfural over titanosilicate catalysts. Green Chemistry, 2017, 19, 4871-4878.	9.0	29
138	Selective hydrogenation of cinnamaldehyde with PtFe /Al2O3@SBA-15 catalyst: Enhancement in activity and selectivity to unsaturated alcohol by Pt-FeO and Pt-Al2O3@SBA-15 interaction. Journal of Catalysis, 2017, 354, 24-36.	6.2	71
139	Eco-Friendly and Cost-Effective Synthesis of ZSM-5 Aggregates with Hierarchical Porosity. Industrial & Engineering Chemistry Research, 2017, 56, 13535-13542.	3.7	29
140	Nickel/USY Catalyst Derived from a Layered Double Hydroxide/Zeolite Hybrid Structure with a High Hydrogenation Efficiency. ChemCatChem, 2017, 9, 4552-4561.	3.7	11
141	Cu 9 -Al x -Mg y catalysts for hydrogenation of ethyl acetate to ethanol. Applied Catalysis A: General, 2017, 544, 108-115.	4.3	11
142	Interfacial Clustering-Triggered Fluorescence–Phosphorescence Dual Solvoluminescence of Metal Nanoclusters. Journal of Physical Chemistry Letters, 2017, 8, 3980-3985.	4.6	79
143	Efficient Pt–FeO <sub>x</sub> /TiO <sub>2</sub> @SBA-15 catalysts for selective hydrogenation of cinnamaldehyde to cinnamyl alcohol. Catalysis Science and Technology, 2017, 7, 6112-6123.	4.1	45
144	ECNU-10 zeolite: A three-dimensional MWW-Type analogue. Microporous and Mesoporous Materials, 2017, 253, 137-145.	4.4	10

HAIHONG WU

#	Article	IF	CITATIONS
145	Liquid-phase oxidation of ethylamine to acetaldehyde oximes over tungsten-doped zeolites. Science China Chemistry, 2017, 60, 942-949.	8.2	6
146	Factors influencing the activity of SiO 2 supported bimetal Pd-Ni catalyst for hydrogenation of α-angelica lactone: Oxidation state, particle size, and solvents. Journal of Catalysis, 2017, 351, 10-18.	6.2	25
147	Hydrophobic Nanosized All-Silica Beta Zeolite: Efficient Synthesis and Adsorption Application. ACS Applied Materials & amp; Interfaces, 2017, 9, 27273-27283.	8.0	77
148	Synthesis of Novel Titanosilicate Catalysts by Simultaneous Isomorphous Substitution and Interlayer Expansion of Zeolitic Layered Silicates. Chemistry of Materials, 2016, 28, 5295-5303.	6.7	26
149	Stabilizing Lowâ€Silica Zeolites through Aluminum Sulfate Assisted Cannibalistic Dealumination. ChemCatChem, 2016, 8, 1891-1895.	3.7	6
150	Postsynthesis of FAU-type stannosilicate as efficient heterogeneous catalyst for Baeyer-Villiger oxidation. Applied Catalysis A: General, 2016, 519, 155-164.	4.3	55
151	Direct synthesis of self-assembled ZSM-5 microsphere with controllable mesoporosity and its enhanced LDPE cracking properties. RSC Advances, 2016, 6, 38671-38679.	3.6	24
152	A mesoporous aluminosilicate prepared by simply coating fibrous γ-AlOOH on the external surface of SBA-15 for catalytic hydrocarbon cracking. RSC Advances, 2016, 6, 40296-40303.	3.6	4
153	Studies on the epoxidation of methallyl chloride over TS-1 microsphere catalysts in a continuous slurry reactor. Catalysis Science and Technology, 2016, 6, 2605-2615.	4.1	20
154	Postsynthesis and Effective Baeyer–Villiger Oxidation Properties of Hierarchical FAU-type Stannosilicate. Journal of Physical Chemistry C, 2016, 120, 23613-23624.	3.1	28
155	A novel acid–base bifunctional catalyst (ZSM-5@Mg <sub>3</sub> Si <sub>4</sub> O <sub>9</sub> (OH) <sub>4</sub> ) with core/shell hierarchical structure and superior activities in tandem reactions. Chemical Communications, 2016, 52, 12817-12820.	4.1	26
156	The superior performance of a Pt catalyst supported on nanoporous SiC–C composites for liquid-phase selective hydrogenation of cinnamaldehyde. RSC Advances, 2016, 6, 81211-81218.	3.6	17
157	Low temperature hydrogenation of α-angelica lactone on silica supported Pd–NiO catalysts with synergistic effect. RSC Advances, 2016, 6, 65377-65382.	3.6	11
158	Isomorphous Incorporation of Tin Ions into Germanosilicate Framework Assisted by Local Structural Rearrangement. ACS Catalysis, 2016, 6, 8420-8431.	11.2	32
159	Self-Assembly of Cetyltrimethylammonium Bromide and Lamellar Zeolite Precursor for the Preparation of Hierarchical MWW Zeolite. Chemistry of Materials, 2016, 28, 4512-4521.	6.7	88
160	Diversity of layered zeolites: from synthesis to structural modifications. New Journal of Chemistry, 2016, 40, 3968-3981.	2.8	44
161	Highly effective Ru/CMK-3 catalyst for selective reduction of nitrobenzene derivatives with H <sub>2</sub> O as solvent at near ambient temperature. RSC Advances, 2016, 6, 3235-3242.	3.6	18
162	Selective synthesis of ethylene oxide through liquid-phase epoxidation of ethylene with titanosilicate/H2O2 catalytic systems. Applied Catalysis A: General, 2016, 515, 51-59.	4.3	43

#	Article	IF	CITATIONS
163	Strong or weak acid, which is more efficient for Beckmann rearrangement reaction over solid acid catalysts?. Catalysis Science and Technology, 2015, 5, 3675-3681.	4.1	32
164	One-pot synthesis of 5-hydroxymethylfurfural from glucose using bifunctional [Sn,Al]-Beta catalysts. Chinese Journal of Catalysis, 2015, 36, 820-828.	14.0	59
165	Preparation of Co- or Mn-substituted LTL zeolites and their catalytic properties in cyclohexane oxidation. Science China Chemistry, 2015, 58, 139-147.	8.2	3
166	Pt nanoparticles entrapped in mesoporous metal–organic frameworks MIL-101 as an efficient catalyst for liquid-phase hydrogenation of benzaldehydes and nitrobenzenes. Journal of Molecular Catalysis A, 2015, 399, 1-9.	4.8	39
167	An insight into crystal morphology-dependent catalytic properties of MOR-type titanosilicate in liquid-phase selective oxidation. Journal of Catalysis, 2015, 325, 101-110.	6.2	34
168	Construction of unique six-coordinated titanium species with an organic amine ligand in titanosilicate and their unprecedented high efficiency for alkene epoxidation. Chemical Communications, 2015, 51, 9010-9013.	4.1	107
169	A hierarchically core/shell-structured titanosilicate with multiple mesopore systems for highly efficient epoxidation of alkenes. Chemical Communications, 2015, 51, 14905-14908.	4.1	32
170	One-pot synthesized hierarchical zeolite supported metal nanoparticles for highly efficient biomass conversion. Chemical Communications, 2015, 51, 15102-15105.	4.1	41
171	Intergrown Zeolite MWW Polymorphs Prepared by the Rapid Dissolution–Recrystallization Route. Chemistry of Materials, 2015, 27, 7852-7860.	6.7	36
172	Amphiphilic Titanosilicates as Pickering Interfacial Catalysts for Liquid-Phase Oxidation Reactions. Journal of Physical Chemistry C, 2015, 119, 25377-25384.	3.1	31
173	Direct synthesis of ordered imidazolyl-functionalized mesoporous polymers for efficient chemical fixation of CO <sub>2</sub> . Chemical Communications, 2015, 51, 682-684.	4.1	49
174	Postsynthesis of mesoporous ZSM-5 zeolite by piperidine-assisted desilication and its superior catalytic properties in hydrocarbon cracking. Journal of Materials Chemistry A, 2015, 3, 3511-3521.	10.3	65
175	Sub-zeolite of FER topology derived from an interlayer modification of PLS-3 lamellar precursor. Microporous and Mesoporous Materials, 2015, 203, 54-62.	4.4	17
176	Post-synthesis and catalytic performance of FER type sub-zeolite Ti-ECNU-8. Chinese Chemical Letters, 2014, 25, 1511-1514.	9.0	16
177	Facile Synthesis of Size Controllable Dendritic Mesoporous Silica Nanoparticles. ACS Applied Materials & Interfaces, 2014, 6, 22655-22665.	8.0	138
178	Post‧ynthesis Treatment gives Highly Stable Siliceous Zeolites through the Isomorphous Substitution of Silicon for Germanium in Germanosilicates. Angewandte Chemie - International Edition, 2014, 53, 1355-1359.	13.8	83
179	Ru Nanoparticles Entrapped in Ordered Mesoporous Carbons: An Efficient and Reusable Catalyst for Liquid-Phase Hydrogenation. Catalysis Letters, 2014, 144, 268-277.	2.6	24
180	Acid strength controlled reaction pathways for the catalytic cracking of 1-butene to propene over ZSM-5. Journal of Catalysis, 2014, 309, 136-145.	6.2	145

#	Article	IF	CITATIONS
181	Distinctions of hydroxylamine formation and decomposition in cyclohexanone ammoximation over microporous titanosilicates. Journal of Catalysis, 2014, 309, 1-10.	6.2	51
182	A Career in Catalysis: Takashi Tatsumi. ACS Catalysis, 2014, 4, 23-30.	11.2	41
183	Influences of fluorine implantation on catalytic performance and porosity of MOR-type titanosilicate. Journal of Catalysis, 2014, 320, 160-169.	6.2	38
184	A highly ordered mesoporous polymer supported imidazolium-based ionic liquid: an efficient catalyst for cycloaddition of CO <sub>2</sub> with epoxides to produce cyclic carbonates. Green Chemistry, 2014, 16, 4767-4774.	9.0	144
185	Pt nanoparticles entrapped in Al2O3@SBA-15 composites: Effective and recyclable catalysts for enantioselective hydrogenation of ethyl 2-oxo-4-phenylbutyrate. Applied Catalysis A: General, 2014, 488, 48-57.	4.3	12
186	Hierarchical, core–shell meso-ZSM-5@mesoporous aluminosilicate-supported Pt nanoparticles for bifunctional hydrocracking. Journal of Materials Chemistry A, 2014, 2, 15535-15545.	10.3	39
187	Bifunctional Tandem Catalysis on Multilamellar Organic–Inorganic Hybrid Zeolites. ACS Catalysis, 2014, 4, 2959-2968.	11.2	64
188	Photoemission Mechanism of Water-Soluble Silver Nanoclusters: Ligand-to-Metal–Metal Charge Transfer vs Strong Coupling between Surface Plasmon and Emitters. Journal of the American Chemical Society, 2014, 136, 1686-1689.	13.7	224
189	Selective synthesis of dimethyl ketone oxime through ammoximation over Ti-MOR catalyst. Applied Catalysis A: General, 2014, 488, 86-95.	4.3	30
190	Preparation of hierarchical MWW-type titanosilicate by interlayer silylation with dimeric silane. Microporous and Mesoporous Materials, 2014, 189, 41-48.	4.4	34
191	Clean Synthesis of Amides over Bifunctional Catalysts of Rhodiumâ€Loaded Titanosilicates. ChemCatChem, 2013, 5, 2462-2470.	3.7	12
192	Clean synthesis of acetaldehyde oxime through ammoximation on titanosilicate catalysts. Catalysis Science and Technology, 2013, 3, 2587.	4.1	29
193	Mesopolymer modified with palladium phthalocyaninesulfonate as a versatile photocatalyst for phenol and bisphenol A degradation under visible light irradiation. Journal of Environmental Sciences, 2013, 25, 1687-1695.	6.1	13
194	Post-synthesis, characterization and catalytic properties of fluorine-planted MWW-type titanosilicate. Physical Chemistry Chemical Physics, 2013, 15, 4930.	2.8	55
195	Enhanced catalytic activity of titanosilicates controlled by hydrogen-bonding interactions. Chemical Communications, 2013, 49, 7504.	4.1	19
196	Facile Large-Scale Synthesis of Monodisperse Mesoporous Silica Nanospheres with Tunable Pore Structure. Journal of the American Chemical Society, 2013, 135, 2427-2430.	13.7	439
197	Post-synthesis and adsorption properties of interlayer-expanded PLS-4 zeolite. Microporous and Mesoporous Materials, 2013, 169, 88-96.	4.4	29
198	Pt nanoparticles supported on highly dispersed TiO2 coated on SBA-15 as an efficient and recyclable catalyst for liquid-phase hydrogenation. Journal of Catalysis, 2013, 300, 9-19.	6.2	67

#	Article	lF	CITATIONS
199	Hydrothermal synthesis of MWW-type stannosilicate and its post-structural transformation to MCM-56 analogue. Microporous and Mesoporous Materials, 2013, 165, 210-218.	4.4	40
200	Preparation of Interlayer-Expanded Zeolite from Lamellar Precursor Nu-6(1) by Silylation. Chemistry of Materials, 2013, 25, 4710-4718.	6.7	37
201	Ordered Mesoporous Carbons with Ia3d Symmetry Supported Pt Catalyst for Efficient Asymmetric Hydrogenation. Catalysis Letters, 2012, 142, 1033-1039.	2.6	13
202	Fluorine-planted titanosilicate with enhanced catalytic activity in alkene epoxidation with hydrogen peroxide. Catalysis Science and Technology, 2012, 2, 2433.	4.1	50
203	Synthesis of core–shell structured TS-1@mesocarbon materials and their applications as a tandem catalyst. Journal of Materials Chemistry, 2012, 22, 14219.	6.7	29
204	Enhancement of Alkene Epoxidation Activity of Titanosilicates by Gasâ€Phase Ammonia Modification. Chinese Journal of Chemistry, 2012, 30, 2205-2211.	4.9	6
205	Multilayer structured MFI-type titanosilicate: Synthesis and catalytic properties in selective epoxidation of bulky molecules. Journal of Catalysis, 2012, 288, 16-23.	6.2	98
206	Synthesis and formation mechanism of TS-1@mesosilica core–shell materials templated by triblock copolymer surfactant. Microporous and Mesoporous Materials, 2012, 153, 8-17.	4.4	20
207	Core/shell-structured TS-1@mesoporous silica-supported Au nanoparticles for selective epoxidation of propylene with H2 and O2. Journal of Materials Chemistry, 2011, 21, 10852.	6.7	88
208	Hydrothermal synthesis of high-silica mordenite by dual-templating method. Microporous and Mesoporous Materials, 2011, 145, 80-86.	4.4	32
209	Pt nanoparticles entrapped in ordered mesoporous carbon for enantioselective hydrogenation. Journal of Molecular Catalysis A, 2011, 345, 81-89.	4.8	53
210	Postsynthesis of mesoporous MOR-type titanosilicate and its unique catalytic properties in liquid-phase oxidations. Journal of Catalysis, 2011, 281, 263-272.	6.2	70
211	ETS-10 Supported Au Nanoparticles for Solvent-Free Oxidation of 1-Phenylethanol with Oxygen. Catalysis Letters, 2011, 141, 860-865.	2.6	7
212	One-pot synthesis of highly ordered Ru-containing mesoporous polymers/silica for benzaldehyde hydrogenation. Reaction Kinetics, Mechanisms and Catalysis, 2011, 104, 99-109.	1.7	6
213	An investigation into cyclohexanone ammoximation over Ti-MWW in a continuous slurry reactor. Applied Catalysis A: General, 2011, 394, 1-8.	4.3	57
214	Hydrothermal synthesis of MWW-type analogues using linear-type quaternary alkylammonium hydroxides as structure-directing agents. Microporous and Mesoporous Materials, 2011, 142, 347-353.	4.4	10
215	Selective epoxidation of propylene to propylene oxide with H2 and O2 over Au/Ti-MWW catalysts. Pure and Applied Chemistry, 2011, 84, 561-578.	1.9	13
216	Oxidative Desulfurization of Aromatic Sulfur Compounds over Titanosilicates. ChemCatChem, 2010, 2, 459-466.	3.7	49

#	Article	IF	CITATIONS
217	Pt Nanoparticles Supported on Highly Dispersed Alumina Coated inside SBAâ€15 for Enantioselective Hydrogenation. ChemCatChem, 2010, 2, 1303-1311.	3.7	23
218	Clean synthesis of biodiesel over solid acid catalysts of sulfonated mesopolymers. Science China Chemistry, 2010, 53, 1481-1486.	8.2	18
219	Hydrothermal synthesis of mesoporous titanosilicate with the aid of amphiphilic organosilane. Journal of Porous Materials, 2010, 17, 399-408.	2.6	25
220	Synthesis of ZSM-5 zeolite hollow spheres with a core/shell structure. Journal of Materials Chemistry, 2010, 20, 10193.	6.7	53
221	Ru Nanoparticles Entrapped in Mesopolymers for Efficient Liquid-phase Hydrogenation of Unsaturated Compounds. Catalysis Letters, 2009, 133, 63-69.	2.6	39
222	Structural Characterization of Interlayer Expanded Zeolite Prepared From Ferrierite Lamellar Precursor. Chemistry of Materials, 2009, 21, 2904-2911.	6.7	70
223	Mesopolymer solid base catalysts with variable basicity: preparation and catalytic properties. Journal of Materials Chemistry, 2009, 19, 4004.	6.7	54
224	Alkoxysilylation of Ti-MWW lamellar precursors into interlayer pore-expanded titanosilicates. Journal of Materials Chemistry, 2009, 19, 8594.	6.7	59
225	Mesostructured polymer-supported diphenylphosphine–palladium complex: An efficient and recyclable catalyst for Heck reactions. Catalysis Communications, 2009, 10, 1099-1102.	3.3	29
226	Effective and Reusable Pt Catalysts Supported on Periodic Mesoporous Resols for Chiral Hydrogenation. Catalysis Letters, 2008, 122, 325-329.	2.6	26
227	Post-transformation of MWW-type lamellar precursors into MCM-56 analogues. Microporous and Mesoporous Materials, 2008, 113, 435-444.	4.4	66
228	Unique solvent effect of microporous crystalline titanosilicates in the oxidation of 1-hexene and cyclohexene. Journal of Catalysis, 2008, 256, 62-73.	6.2	142
229	Preparation of active and robust palladium nanoparticle catalysts stabilized by diamine-functionalized mesoporous polymers. Chemical Communications, 2008, , 6297.	4.1	64
230	Synthesis, Crystallization Mechanism, and Catalytic Properties of Titanium-Rich TS-1 Free of Extraframework Titanium Species. Journal of the American Chemical Society, 2008, 130, 10150-10164.	13.7	326
231	Methodology for Synthesizing Crystalline Metallosilicates with Expanded Pore Windows Through Molecular Alkoxysilylation of Zeolitic Lamellar Precursors. Journal of the American Chemical Society, 2008, 130, 8178-8187.	13.7	216
232	Highly efficient epoxidation of propylene over a novel Ti-MWW catalyst. Studies in Surface Science and Catalysis, 2007, , 1236-1243.	1.5	12
233	Hydrothermal synthesis of boron-free Ti-MWW with dual structure-directing agents. Studies in Surface Science and Catalysis, 2007, , 464-469.	1.5	24
234	Epoxidation of 2,5-dihydrofuran to 3,4-epoxytetrahydrofuran over Ti-MWW catalysts. Applied Catalysis A: General, 2007, 320, 173-180.	4.3	16

HAIHONG WU

#	Article	IF	CITATIONS
235	Highly selective synthesis of methyl ethyl ketone oxime through ammoximation over Ti-MWW. Applied Catalysis A: General, 2007, 327, 22-31.	4.3	52
236	Highly efficient and clean synthesis of 3,4-epoxytetrahydrofuran over a novel titanosilicate catalyst, Ti-MWW. Green Chemistry, 2006, 8, 78-81.	9.0	13
237	Preparation of Mesoporous Molecular Sieves Al-MSU-S Using Ionic Liquids as Template. Chinese Journal of Chemistry, 2006, 24, 1282-1284.	4.9	8
238	Structure Elucidation of the Highly Active Titanosilicate Catalyst Ti-YNU-1. Angewandte Chemie - International Edition, 2005, 44, 6719-6723.	13.8	73
239	Synthesis of Ti-MWW by a dry-gel conversion method. Catalysis Today, 2005, 99, 233-240.	4.4	44
240	Influence of Fluorine on the Catalytic Performance of Tiâ^'Beta Zeolite. Journal of Physical Chemistry B, 2004, 108, 4242-4244.	2.6	31
241	A Titanosilicate That Is Structurally Analogous to an MWW-Type Lamellar Precursor. Angewandte Chemie - International Edition, 2004, 43, 236-240.	13.8	162
242	Delamination of Ti-MWW and High Efficiency in Epoxidation of Alkenes with Various Molecular Sizes. Journal of Physical Chemistry B, 2004, 108, 19126-19131.	2.6	140
243	A novel titanosilicate with MWW structureCatalytic properties in selective epoxidation of diallyl ether with hydrogen peroxide. Journal of Catalysis, 2004, 228, 183-191.	6.2	68
244	Uniquetrans-Selectivity of Ti-MWW in Epoxidation ofcis/trans-Alkenes with Hydrogen Peroxide. Journal of Physical Chemistry B, 2002, 106, 748-753.	2.6	67
245	Postsynthesis, Characterization, and Catalytic Properties in Alkene Epoxidation of Hydrothermally Stable Mesoporous Ti-SBA-15. Chemistry of Materials, 2002, 14, 1657-1664.	6.7	211
246	Preparation of B-free Ti-MWW through reversible structural conversion. Chemical Communications, 2002, , 1026-1027.	4.1	103
247	Extremely high trans selectivity of Ti-MWW in epoxidation of alkenes with hydrogen peroxide. Chemical Communications, 2001, , 897-898.	4.1	50
248	A dramatic improvement of epoxide selectivity of [Ti,Al]-beta by ion-exchange with quaternary ammonium salts. Chemical Communications, 2001, , 1714-1715.	4.1	12
249	A Novel Titanosilicate with MWW Structure. I. Hydrothermal Synthesis, Elimination of Extraframework Titanium, and Characterizations. Journal of Physical Chemistry B, 2001, 105, 2897-2905.	2.6	328
250	A Novel Titanosilicate with MWW Structure: II. Catalytic Properties in the Selective Oxidation of Alkenes. Journal of Catalysis, 2001, 202, 245-255.	6.2	239
251	Hydrothermal Synthesis of a Novel Titanosilicate with MWW Topology. Chemistry Letters, 2000, 29, 774-775.	1.3	86
252	Hydroxylation of Aromatics with Hydrogen Peroxide over Titanosilicates with MOR and MFI Structures:Â Effect of Ti Peroxo Species on the Diffusion and Hydroxylation Activity. Journal of Physical Chemistry B, 1998, 102, 9297-9303.	2.6	71

#	Article	IF	CITATIONS
253	Ammoximation of Ketones over Titanium Mordenite. Journal of Catalysis, 1997, 168, 400-411.	6.2	113
254	Characterization of Titanium Species Incorporated into Dealuminated Mordenites by Means of IR Spectroscopy and 180-Exchange Technique. The Journal of Physical Chemistry, 1996, 100, 10316-10322.	2.9	123
255	Acidic and catalytic properties of aluminated mordenite zeolite: effect of extraframework aluminium. Journal of the Chemical Society, Faraday Transactions, 1996, 92, 861.	1.7	21
256	IR and MAS NMR Studies on the Incorporation of Aluminum Atoms into Defect Sites of Dealuminated Mordenites. The Journal of Physical Chemistry, 1995, 99, 10923-10931.	2.9	96
257	Synthesis and interlayer structure reconstruction of a new layered zeolitic aluminosilicate. Journal of Porous Materials, 0, , .	2.6	0